Tracing and quantification of pharmaceuticals using MR imaging and spectroscopy at clinical MRI system

Eun-Kee Jeong[*a], Xin Liu[b], Xianfeng Shi[c], Y. Bruce Yu[d], Zeng-Rong Lu[e]

[a]Dept. of Radiology and Utah Center for Advanced Imaging Research, [c]Dept. of Psychiatry, and [a,c]Utah Brain Institute, Univ. of Utah, Salt Lake City, UT 84108, USA
[b]Dept. of Radiology & Biomedical, Univ. of California, San Francisco, CA 94143, USA
[d]Dept. of Pharmaceutical Science, University of Maryland, Baltimore, MD 21021, USA
[e]Dept. of Bioengineering, Case Western Reserve University, Cleveland, OH, USA

[*]e-mail: ekj@ucair.med.utah.edu, UCAIR, 729 Arapeen Drive, Salt Lake City, UT 84108, USA

Abstract

Magnetic resonance imaging (MRI) and spectroscopy (MRS) is very powerful modality for imaging and localized investigation of biological tissue. Medical MRI measures nuclear magnetization of the water protons, which consists of 70 % of our body. MRI provides superior contrast among different soft tissues to all other existing medical imaging modalities, including ultrasound, X-ray CT, PET, and SPECT. In principle, MRI/S may be an ideal non-invasive tool for drug delivery research. However, because of its low sensitivity, a large dose is required for tracing pharmaceuticals. Therefore, its use for imaging of pharmaceuticals is very limited mostly to molecules that contain a paramagnetic metal ion, such as gadolinium (Gd^{3+}) and manganese (Mn^{2+}). The paramagnetic metal ion provides a large fluctuating magnetic field at the proton in the water molecule via a coordinate site. The measurement of local drug concentration is the first step for further quantification. Local concentration of the paramagnetic-ion based MRI contrast agent can be indirectly measured via the change in the water signal intensity. ^{19}F MRI/S of fluorinated complex may be an option for drug delivery and tracing agent, because the fluorinated molecule may be directly detected due to its large magnetic moment (94 % of proton) and 100 % abundance.

Keywords: MR Imaging, MR spectroscopy, drug tracing, drug delivery

INTRODUCTION

Traditional population pharmacokinetic (PK) study requires sacrificing a large number of animals at various time points. The organs are extracted, and the concentration of the drug in organs is then determined *in vitro*, using assays such as high-performance liquid chromatography (HPLC). Such a PK study is based on the assumption that all the animals sacrificed at different time points have the same biological conditions. The degree, to which this assumption is violated, may introduce considerable variance in the PK parameters extracted from the data. For *in vivo* experiments, only plasma or excreted drug concentration is normally accessible, but not tissue concentration. Plasma levels of compound often differ from concentrations in specific tissues. The drug concentration in specific tissue won't be the same as that in the plasma (1).

In-vivo tracing of the pharmaceuticals can provide various advantages in drug developments, particularly for personalized medicine. Various physiological parameters can be measured using the precise concentration of the drug within a specific organ. Dynamic-Contrast-Enhanced MRI (DCE MRI) with a paramagnetic contrast agent is commonly used to study in-vivo blood perfusion (2-3), because of its high sensitivity. Paramagnetic ions can reduce the spin-lattice relaxation time (T_1) of water proton NMR at low concentration; as a result, T_1-weighted images show enhanced signal intensities in the vicinity of paramagnetic ions. The higher the local concentration of paramagnetic ions is, the larger the enhancement of the signal intensity is. In fact, the paramagnetic metal ion induces the decreases in both T_1 and T_2. At low concentration, the signal change is mainly due to the change in T_1.

Non-proton MRI has rarely been used to study pharmacokinetics, because its signal intensity is generally very low. Although hyperpolarized gas (^3He or ^{129}Xe) MRI can provide high signal intensity, and therefore high temporal resolution, the short life-time (about 30 sec) o[i]f *in vivo* hyperpolarized gas limits the observation window. Also because the same flipangle is generally used at each time point, magnetization tipped to the transverse plane to generate the signal varies from one time point to another, making it hard to quantify tracer concentration over different time points. ^{19}F MRI/S is a possible option, although its signal intensity cannot be compared to hyperpolarized gas. It has high

Nanosystems in Engineering and Medicine, edited by Sang H. Choi, Jin-Ho Choy, Uhn Lee, Vijay K. Varadan,
Proc. of SPIE Vol. 8548, 854845 · © 2012 SPIE · CCC code: 1605-742/12/$18 · doi: 10.1117/12.1000015

gyromagnetic ratio compared to other non-^{1}H nuclei, no background signal, 100 % abundance, and reusable magnetization (unlike hyperpolarized magnetization). ^{19}F MRI/S have been used to study a variety of biologic processes including metabolism (4-6), tumor growth (7-9), blood flow (10-11) and cell tracking (12). However, most fluorinated compounds are not for *in vivo* ^{19}F MRI applications because of their low signals, multiple peak that result in further signal loss, long T_1, and long retention time *in vivo* due to the high hydrophobicity or water solubility. ^{19}F MR spectroscopy has been used to investigate the clearance of corticosteroid drug (triamcinolone acetonide phosphate) in the eye (13), delivery of psychiatric drugs, e.g. trifluorinated neuroleptics (fluphenazine and trifluoperazine) and trifluorinated antidepressants (fluoxetine and fluvoxamine) (14) and anticancer drugs, e.g. 5-FU (15-16).

In this presentation, three MRI/S applications will be presented for tracing and quantification of the exogenous pharmaceuticals, which were performed at a clinical MRI system with 3T magnetic field strength. Requirements to improve the measurement sensitivity are also discussed.

METHODS AND MATERIALS

All MR experiments were performed at a 3T clinical wholebody MRI system (Tim-Trio, Siemens Medical Solution, Erlangen, Germany). Anatomy and animal specific RF coils were developed for each work. Pulse sequences were developed at IDEA, pulse sequence development environment for Siemens MRI system.

RF coil for small animal MRI: Higher resolution is needed to image a small animal, which requires increased sensitivity for adequate signal-to-noise ratio (SNR). RF coil is an antenna that allows communication between the spectrometer and the spin system. It transmits electromagnetic wave during RF pulse to and receives NMR signal from the spin-system. The transverse magnetization induces electromotive force (emf) on the RF coil. However, all RF coils for human applications are too large for imaging small animal. The sensitivity of an RF coil depends on the filling factor of the imaging object within the effective coil volume. Thus, the clinical RF coil loose the sensitivity for small animal MR imaging because of low filling factor.

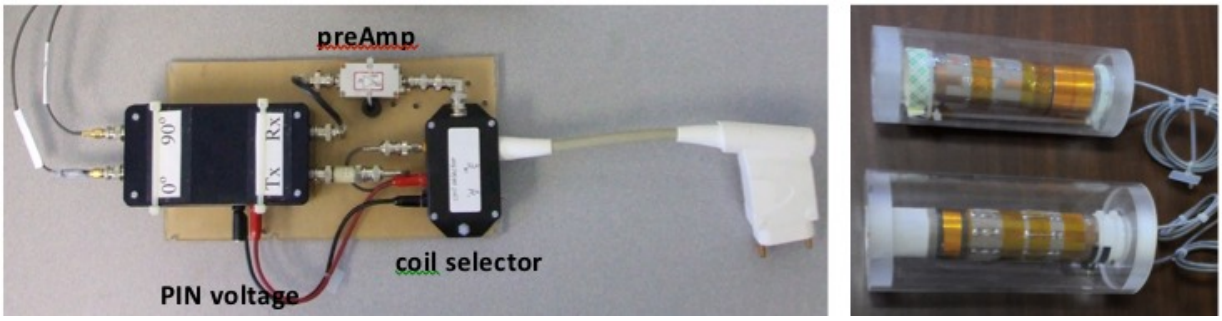

Figure 1. *(a) Quadrature T/R switch, including preamplifier and (b) two single tuned quadrature RF coils for mouse imaging. A PIN diode is used to switch between Tx and Rx in T/R switch. T/R switch is capable to accept a proton-only or ^{19}F/^{1}H dualtune RF coil.*

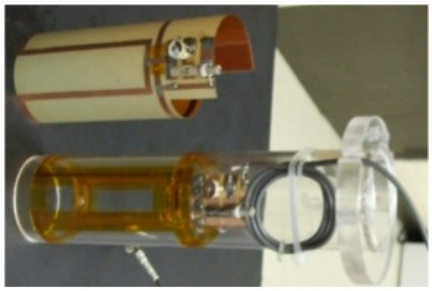

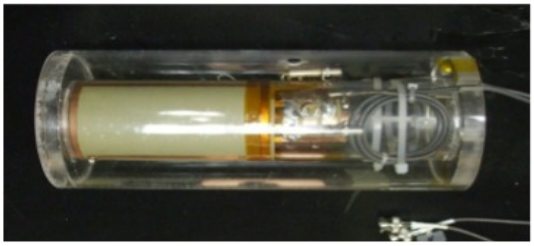

Figure 2. *(a) Two saddle coils. ^{1}H coil was printed on a copper plated microwave circuit board. (b) Two coils combined.*

Transmit/receive (T/R) switch, shown in Fig. 1a, is used to direct the RF pulse from the RF amplifier to the coil and NMR signal from the coil to the preamplifier/receiver. It protects the preamplifier from the high-power RF pulse. It can be built or purchased from coil manufactures. For ^{1}H-only MR imaging, it can be Tx/Rx volume type or receive-only phased array surface coil using the body RF coil for RF transmission. For the quantification of the drug-delivery research, volume RF coil is preferred because of its superior RF homogeneity to that of surface RF coil. Fig. 2 shows a ^{19}F/^{1}H dualtune RF coil for mouse imaging.

One practical problem to build a $^{19}F/^{1}H$ dualtune coil is that their resonance frequencies at 3T are separated only 7 MHz. It is generally difficult to make a dualtune RF resonator with single physical coil for two frequencies with such small separation. One possible option is to utilize the PIN diode to switch between two resonance frequencies. The coil is constructed for ^{1}H resonance and capacitors are added for lower ^{19}F frequency to specific positions in the coil with PIN diodes. Using the PIN diode control logic, that modern MRI system provides, the coil can be tuned and matched for either ^{1}H or ^{19}F frequency in runtime. In our ^{19}F MRI project, a double-tuned $^{19}F/^{1}H$ RF coil was constructed using two saddle coils, one for ^{19}F and another for ^{1}H, which are geometrically positioned orthogonal to each other. It is necessary to null the mutual inductance between two coils. Further fine adjustments, which include tuning, matching, and coil decoupling, were accomplished using variable capacitors in the coil.

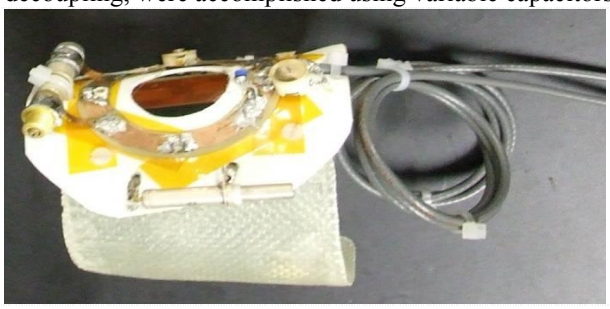

Figure 3. *^{19}F single-tuned quadrature RF coil with T/R switch in Fig. 1(a) for rabbit eye ^{19}F MR spectroscopy, consisting of a circular and 8-shaped coils to orient the magnetic field orthogonal to each other. The coil is positioned within a volume Tx/Rx coil. ^{1}H coil was actively detuned during the ^{19}F imaging by PIN diodes.*

MRI and MRS pulse sequences

Clinical MRI system includes very stable pulse sequences for routine patient examinations. However, typical clinical pulse sequences may not run for MRI and MRS of nuclei other than proton or some of the imaging parameters may not be suitable for small animal imaging. It may be necessary to either modify or make major changes in the source code and recompile and install the binaries into the MRI system.

FID sequence for MR spectroscopy using a surface Tx/Rx coil: Surface RF coil is used to improve the SNR by limiting the noise. It generates the very inhomogeneous, i.e. spatially variant, RF pulse and correspondingly its reception sensitivity is also spatially variant. This spatial inhomogeneity is often used for localization. However, it is the barrier for the quantification for MR image based PK study. Adiabatic RF pulse, such as adiabatic half passage or BIR4 (B_1 Independent Rotation), can be used as the excitation RF pulse to improve the spatial homogeneity. These waveforms with time-varying amplitude and phase need to be generated either externally and imported into the sequence, or internally within the pulse sequence. The sequence (b) was used to study the clearance of TAP (triamcinolone acetonide phosphate, $C_{24}H_{31}FO_6$, 637 g/mol) in rabbit eye. TAP contains a ^{19}F nucleus in a molecule.

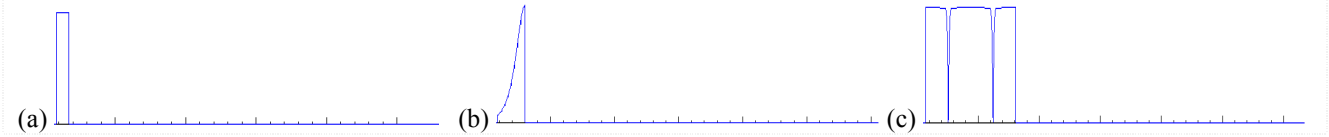

Figure 4. *Single-pulse FID pulse sequence with (a) rectangular, (b) adiabatic half passage (AHP), and (c) BIR4 excitation. The adiabatic RF excitation in (b, c) not only helps improve the RF homogeneity within the effective volume of a surface coil, also improve the SNR.*

Gradient-echo pulse sequence with short TE for density-weighted ^{19}F MRI: For quantification PK study, it is necessary to measure the MR images without other weighting, such as T_1 or T_2 weighting. The echotime TE must be minimal with the recovery time (TR) larger than 3 T_1. Pulse sequence diagram in Fig. 5a and 5b indicate a gradient-echo imaging sequence with (a) asymmetric and (b) symmetric excitation RF pulses. TE is reduced by 1.1 ms using the asymmetric RF pulse. Reduction of TE by 1.1 ms may be a significant for imaging of short T_2 species such as imaging Gd-chelated ^{19}F complex. This sequence was used for ^{19}F MRI of ^{19}FIT (fluorinated imaging tracer).

MRI and MRS experiments: All animal MRI experiments were performed under the protocol, approved by the Institutional Animal Care and Usage Committee (IACUC) of the University of Utah. The animals were anaesthetized using a cocktail of Ketamine and Xylazine with appropriate dose. Body temperature was maintained at about 36 ^{o}C by supplying warm air directly to around the animal body. Each RF coil was tuned and matched, before placing the animal into the RF coil.

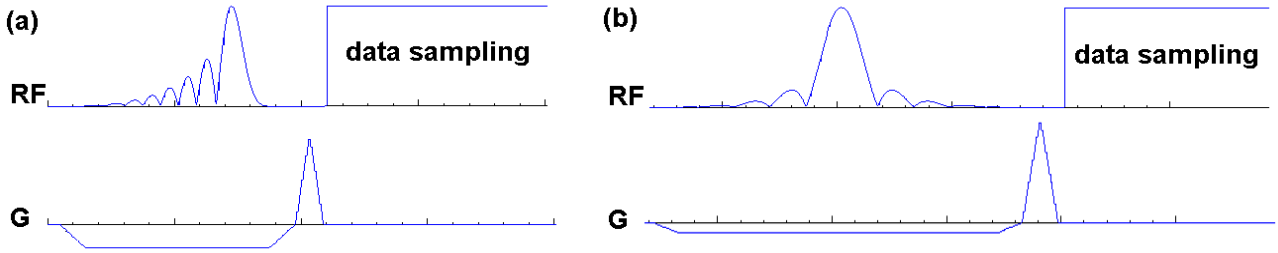

Figure 5. *Gradient-echo imaging pulse sequence with (a) asymmetric and (b) symmetric excitation RF pulses with the corresponding echotimes 1.0 and 2.1 ms, respectively. The reduced TE in (a) will help in reducing error in density-weighted MRI. The asymmetric RF allows reducing the effective dephasing time during the excitation and correspondingly the refocusing duration as well, thus the TE becomes shorter. Rectangular box in RF line indicates the data acquisition window.*

RESULTS

Proton MRI of gadolinium-based contrast agent: Dr. Lu, one of the authors, is an expert to develop various polymerized MR imaging and drug delivery agents. We have been intensively developed and investigated pharmacokinetics of these new MRI agents on mice using MRI (17-26). One set of dynamic MR images is shown in Fig. 6 from mice injected with polymerized Gd complex with different molecular weights (top: 21 kDa, mid: 60 kDa) at different time points. These images were acquired using a home-made mouse volume RF coil, which gave 3 times SNR improvement compared with that using a human wrist RF coil. The plots on the right indicate the signal intensity/time curves of blood plasma and ROIs at liver and kidney, respectively.

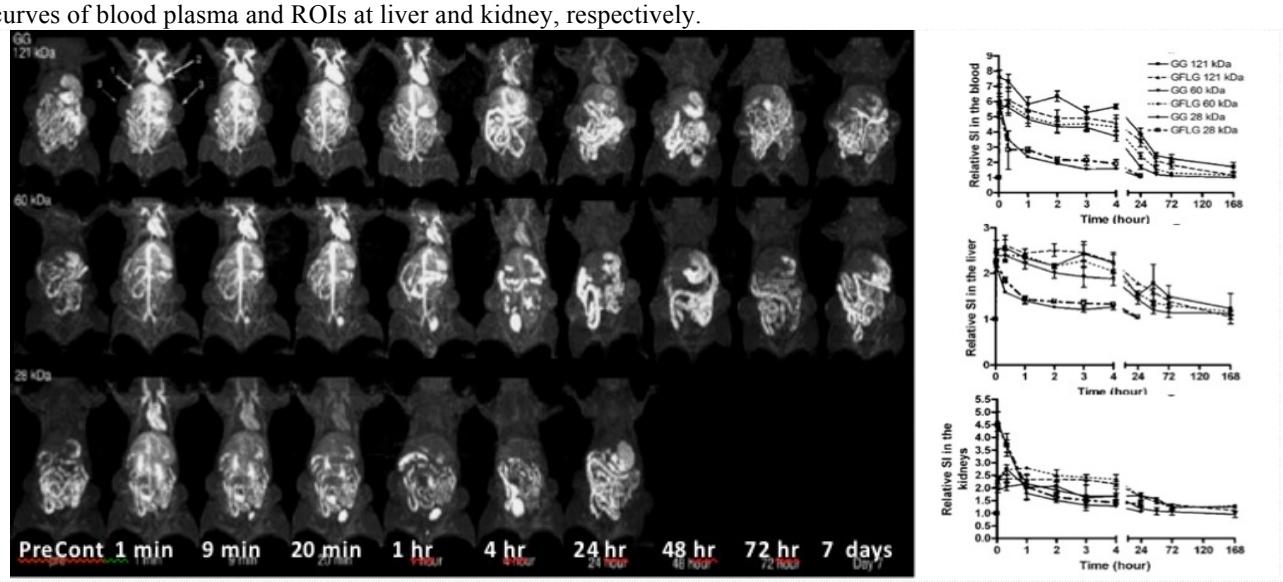

Figure 6. (Lt) *Dynamic MR images of mice with polymerized Gd complex injected and (Rt) time course of the signal intensity at blood, liver, and kidney.*

Proton-MRI for rabbit eye study: GBCA (Gd-based contrast agent) aided proton imaging experiment were performed on rabbit eyes with various compounds with different molecular weights (~ 144 kDa) (27), which were developed by Dr. Lu's group. Clinical GBCA (MultiHance), which has a low molecular weight, was injected into opposite eye as the control. The purpose of the study was to evaluate the effect of molecular sizes upon the clearance of drugs in the eye. The clearance of these molecules is expected to be dominated by the physical diffusion of the molecules in the vitreous humor at early time points and then by the blood circulation after the molecules reach the tissue. T_1 weighted spin-echo images using conventional spin-echo and rapid T_1 mapping using a multishot-EPI with automated TR and TE (27) were acquired at each time point. Because of the lack of active carriers in the eye, the molecular transport relies on self-diffusive motion of the drug compounds until the molecules reach the tissues surrounding the vitreous humor. Fig. 7 (a, b) are T_1 weighted images, and (c, d) are their corresponding concentration maps of selected time points. The concentration maps were calculated using the T_1 maps with known total amount at t = 0.

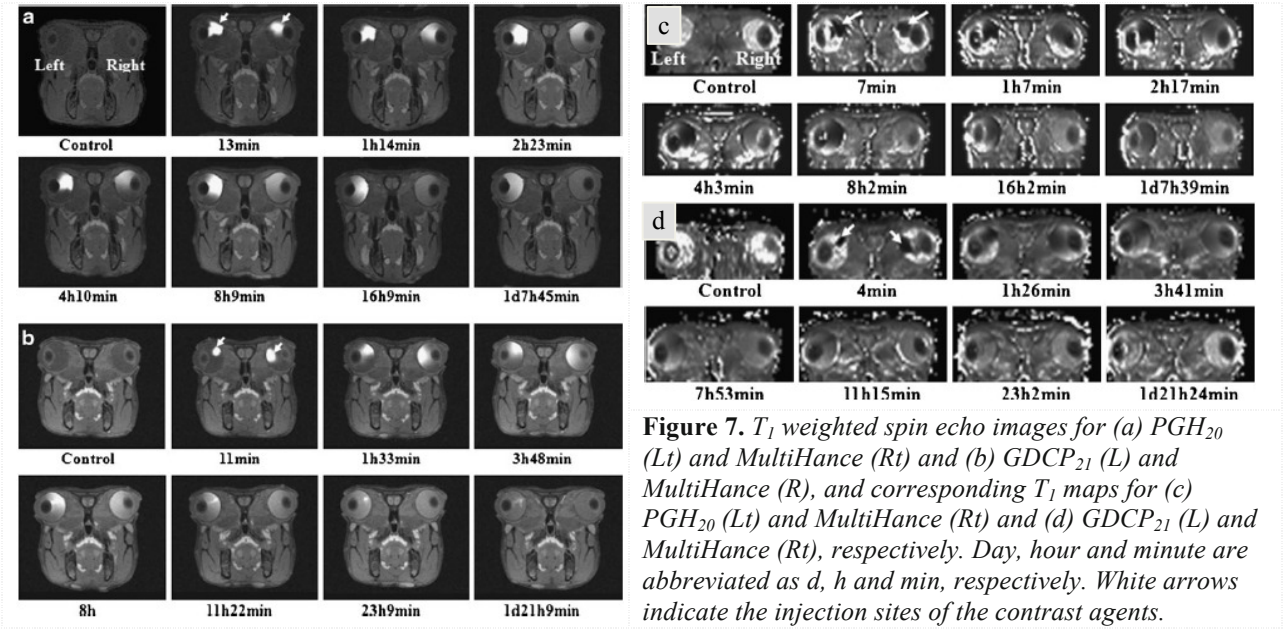

Figure 7. *T_1 weighted spin echo images for (a) PGH_{20} (Lt) and MultiHance (Rt) and (b) $GDCP_{21}$ (L) and MultiHance (R), and corresponding T_1 maps for (c) PGH_{20} (Lt) and MultiHance (Rt) and (d) $GDCP_{21}$ (L) and MultiHance (Rt), respectively. Day, hour and minute are abbreviated as d, h and min, respectively. White arrows indicate the injection sites of the contrast agents.*

The plots in Fig. 8 display the clearance patterns of each compound. The concentration signals within the regions-of-interest (ROIs), which were manually selected, were summed over the entire eye for all slices. Because of the variability to measure T_1 relaxation time in human MRI system, it was difficult to measure the short T_1; hence, T_1 map of the high Gd^{3+} concentration at early time point is subject to error.

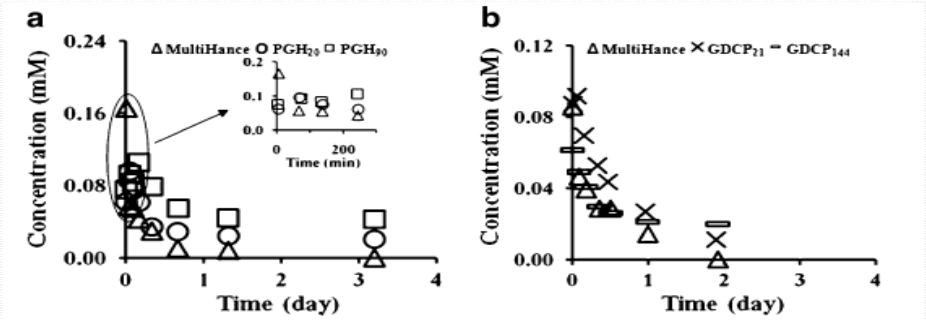

Figure 8. *Concentration-time profile of (a) non-biodegradable PGH (20 and 90 kDa) and (b) biodegradable GDCP (21 and 144 kDa). The concentration-time profiles of MultiHance in (a) and (b) are shown as reference.*

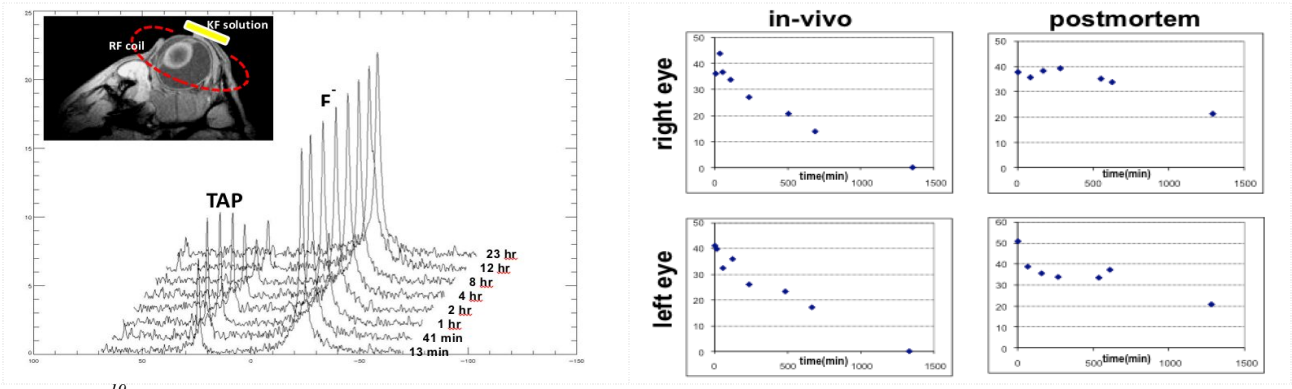

Figure 9. *^{19}F spectra of TAP in rabbit eye, measured at different time points. The inserted figure shows the relative positions of the coil and reference sample with respect to the eye. This result was presented in the article, Liu X, Li KS, Jeong EK, Exp. Eye Res, 2010; 91: 347-352. (Reference 32)*

^{19}F MR spectroscopy for eye study: This experiment was to measure the clearance pattern of a clinical anti-inflammatory drug in the eye (28). Prior to this experiment, paramagnetic-ion based MRI contrast agents were used to mimic the clinical drug, such as TAP and DSP (dexamethasone phosphate), assuming that the clearance pattern in the eye is solely determined by the size of the drug molecules (29-32). In this experiment, the drug molecule was directly observed by ^{19}F MR spectroscopy. While the traditional method requires sacrificing a large number of rabbits at various time points for PK study, only four rabbits were used for the study. Fig. 9 shows the changes of ^{19}F signal intensity on the same animals over time post-injection. As shown in the insert, ^{19}F Tx/Rx coil is position on the same equator plane of the eye, and a reference vial filled with a known quantity of ^{19}F as KF is placed opposite side of the eye to normalize the sensitivity variation of the coil due to different MR loading effect. The plots on the right are the signal-intensity vs. post-injection time for in-vivo and post-mortem rabbits to evaluate the clearance of the TAP. The half-life in the postmortem eye is much longer than that in in-vivo, which indicates the major route for the drug clearance may be affected by blood circulation.

^{19}F MRI: Most of the commercially available fluorinate complexes are handicapped for ^{19}F MRI, by their hydrophobicity, long ^{19}F T_1, small number of ^{19}F nuclei within a molecule, and multiple chemical shift peaks, and thus the detection sensitivity is very low. Dr. Yu's group at University of Maryland has been developing fluorinated imaging/tracing (^{19}FIT) agent (33-34), which contains 27 chemically identical ^{19}F nuclei, a few hundred ms T_1 and low hydrophobicity. Its in-vivo half-life was found to be about 6 hours in mice. It is known that perfluoro-15-crown-5-ether ($C_{10}F_{10}O_5$), most commonly used ^{19}F MRI agent, is cleared through the lung. Fig. 10 shows a series of ^{19}F MR images that are overlaid on anatomic proton MR images. Image at each time point was measured on the same animal, thus variability among the different animals is not a question as in traditional non-image based PK study.

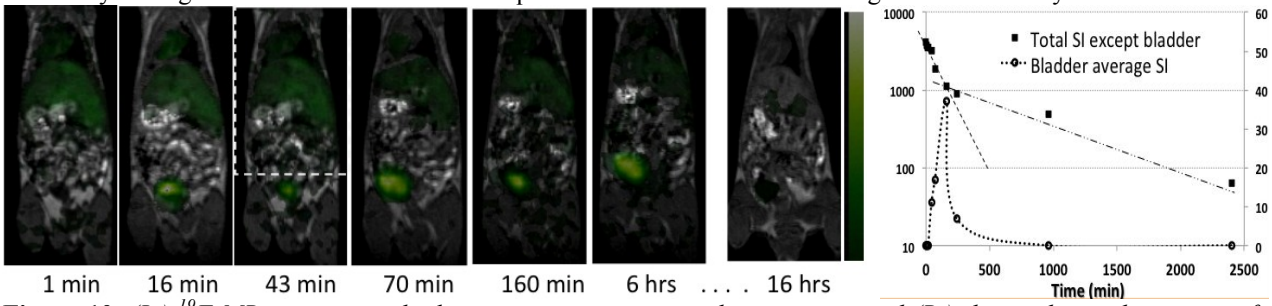

Figure 10. *(Lt) ^{19}F MR images overlaid on proton images at each time point, and (Rt) the total signal intensity of the region-of-interest enclosed within the dotted box shown in 43 min time point. Similar work was presented by Jiang ZX, Liu X, Jeong EK, Yu YB, Angew. Chem. Int., 2009, 48, 4755. (See reference 33).*

DISCUSSION

For pharmacokinetic evaluation of specific pharmaceuticals, it is important to accurately estimate the local concentration of the drug molecules. Although paramagnetic-ion based molecules, such as Gd^{2+} and Mn^{2+}, are most commonly used as the MR imaging and delivery agents, the signal intensity of the water proton MRI, assisted by these contrast agents, is not linear with the local concentration of the metal ions, as shown in Fig. 9. Rather, the spin-lattice relaxation rate R_1 (= $1/T_1$) is linear to the concentration as $R_1(C) = \frac{1}{T_{10}} + r_1 C$, where r_1 is defined as the relaxivity of the agent molecule (35-36). It takes several minutes or longer to measure T_1 relaxation time using conventional MR imaging method, thus it is not practical to use the T_1 to estimate the local concentration of the metal ions, particularly in dynamic MR imaging. In most dynamic perfusion MR imagings, the signal intensity is converted using a calibration method with phantom data obtained in a separate experiment. However, the relaxivity of the paramagnetic-ion based MRI contrast agent differs in tissue from that in solution in the phantom due to the different molecular motion, particularly the rotational motion. Systematic errors are introduced during the conversion of the signal intensity to the local concentration, and these errors propagate to all resultant PK evaluations. Rapid T_1 map imaging can be used for dynamic perfusion imaging for PK analysis (27, 37, 38).

In contrast to GD-assisted proton MRI, the signal-intensity of the density-weighted ^{19}F MRI/S is linear with the ^{19}F concentration. However, even with a large number of ^{19}F atoms in a molecule, relatively short T_1, and a single resonance peak, the sensitivity of the ^{19}F imaging agent is generally low. Therefore, increased dose is required. Fortunately, most fluorinated complex is chemically very stable and relatively safe for in-vivo usage. In case that the MR imaging is not

sensitive enough to evaluate the kinetics of the fluorinated complex, a localized ^{19}F MR spectroscopy with increased voxel dimension can be used to measure the fluorinated molecules within a specific organ.

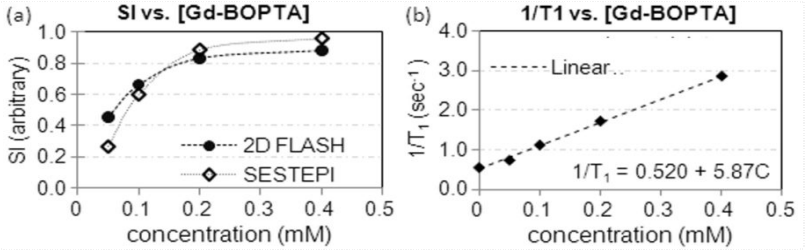

Figure 11. *(a) Signal intensities of spin-echo and gradient-echo images, and (b) $1/T_1$ vs. [Gd(III)] in a solution phantom with various concentrations. Dotted line in (b) indicates linear fit to $1/T_1$ with $1/T_{10}$ = 0.520 sec^{-1}, and relaxivity r_1=5.87 $sec^{-1}.mM^{-1}$.*

It is advantageous to conduct mouse/rat MRI using a small bore animal MRI system. Because the organs in rodents are proportionally small compared to those in human, spatial resolution must be correspondingly increased. But it is relatively less available. An alternative approach is to use the wholebody clinical MRI system, which is widely available at almost every major hospital. One definite advantage using a clinical MRI system for drug development study is that we may be able to evaluate the sensitivity of the future practical application. For instance, a fluorinated compound may give the signal intensity sufficient for PK evaluation at 7 T MRI system, but not at the clinical MRI system with lower magnetic field strength.

Although the spatial resolution can be improved using a higher field magnet, the relaxivity of a paramagnetic-ion based MR imaging/tracing agent is different at high field compared with that in the low field of clinical MRI system. In this sense, it is preferred to perform MRI experiment with high-filling factor animal MRI RF coil at the field strength comparable to that for human MRI system, such as 1.5 and 3 T systems. However, compared with small-bore research MRI systems, it is much more complex for pulse sequence programming at the clinical MRI system. This complexity in a clinical MRI system is mostly from various imaging options and the intensive safety check.

Acknowledgement: This work was partially supported by NSF CBET 1133908.

REFERENCES

[1] Reid DG, Murphy PS. Fluorine magnetic resonance in vivo: a powerful tool in the study of drug distribution and metabolism. Drug Discov Today 2008;13(11-12):473-480.

[2] Kim SH, Csaky KG, Wang NS, Lutz RJ. Drug elimination kinetics following subconjunctival injection using dynamic contrast-enhanced magnetic resonance imaging. Pharm Res 2008;25(3):512-520.

[3] Wang Y, Ye F, Jeong EK, Sun Y, Parker DL, Lu ZR. Noninvasive visualization of pharmacokinetics, biodistribution and tumor targeting of poly[N-(2-hydroxypropyl)methacrylamide] in mice using contrast enhanced MRI. Pharm Res 2007;24(6):1208-1216.

[4] Klomp D, van Laarhoven H, Scheenen T, Kamm Y, Heerschap A. Quantitative 19F MR spectroscopy at 3 T to detect heterogeneous capecitabine metabolism in human liver. NMR Biomed 2007;20(5):485-492.

[5] Schneider E, Bolo NR, Frederick B, et al. Magnetic resonance spectroscopy for measuring the biodistribution and in situ in vivo pharmacokinetics of fluorinated compounds: validation using an investigation of liver and heart disposition of tecastemizole. J Clin Pharm Ther 2006;31(3):261-273.

[6] van Laarhoven HW, Punt CJ, Kamm YJ, Heerschap A. Monitoring fluoropyrimidine metabolism in solid tumors with in vivo (19)F magnetic resonance spectroscopy. Crit Rev Oncol Hematol 2005;56(3):321-343.

[7] Porcari P, Capuani S, D'Amore E, et al. In vivo 19F MR imaging and spectroscopy for the BNCT optimization. Appl Radiat Isot 2009;67(7-8 Suppl):S365-368.

[8] Procissi D, Claus F, Burgman P, et al. In vivo 19F magnetic resonance spectroscopy and chemical shift imaging of tri-fluoro-nitroimidazole as a potential hypoxia reporter in solid tumors. Clin Cancer Res 2007;13(12):3738-3747.

[9] Ramaprasad S, Ripp E, Missert J, Pandey RK. In vivo 19F MR studies of fluorine labeled photosensitizers in a murine tumor model. Curr Drug Discov Technol 2007;4(2):126-132.

[10] Ligeti L, Pekar J, Ruttner Z, McLaughlin AC. Determination of cerebral oxygen consumption and blood flow by magnetic resonance imaging. Acta Biomed Ateneo Parmense 1995;66(3-4):67-74.

[11] van Zijl PC, Ligeti L, Sinnwell T, et al. Measurement of cerebral blood flow by volume-selective 19F NMR spectroscopy. Magn Reson Med 1990;16(3):489-495.

[12] Janjic JM, Ahrens ET. Fluorine-containing nanoemulsions for MRI cell tracking. Wiley Interdiscip Rev Nanomed Nanobiotechnol 2009;1(5):492-501.
[13] Liu X, Kevin Li S, Jeong EK. Ocular pharmacokinetic study of a corticosteroid by 19F MR. Exp Eye Res 2010;91(3):347-352.
[14] Bartels M, Albert K. Detection of psychoactive drugs using 19F MR spectroscopy. J Neural Transm Gen Sect 1995;99(1-3):1-6.
[15] Kamm YJ, Heerschap A, van den Bergh EJ, Wagener DJ. 19F-magnetic resonance spectroscopy in patients with liver metastases of colorectal cancer treated with 5-fluorouracil. Anticancer Drugs 2004;15(3):229-233.
[16] Dresselaers T, Theys J, Nuyts S, et al. Non-invasive 19F MR spectroscopy of 5-fluorocytosine to 5-fluorouracil conversion by recombinant Salmonella in tumours. Br J Cancer 2003;89(9):1796-1801.
[17] Tan M, Ye Z, Jeong EK, Wu X, Parker D, Lu ZR. Synthesis and Evaluation of Nanoglobular Macrocyclic Mn(II) Chelate Conjugates As Non-Gadolinium(III) MRI Contrast Agents., Bioconjug Chem. 2011; 22(5): 931-937
[18] Wang Y, Ye F, Jeong EK, Sun Y, Parker DL, Lu ZR., Noninvasive visualization of pharmacokinetics, biodistribution and tumor targeting of poly[N-(2-hydroxypropyl)methacrylamide] in mice using contrast enhanced MRI. Pharm Res. 2007, 24(6):1208-16.
[19] Xu R, Kaneshiro TL, Jeong EK, Parker DL, and Lu ZR, Synthesis and evaluation of nanoglobule-cystamine-(Gd-DO3A), a biodegradable nanosized magnetic resonance contrast agent for dynamic contrast-enhanced magnetic resonance urography, Int J Nanomedicine. 2010, 5:707-13.
[20] Wang Y, Ye F, Jeong EK, Sun Y, Parker DL, Lu ZR., Noninvasive visualization of pharmacokinetics, biodistribution and tumor targeting of poly[N-(2-hydroxypropyl)methacrylamide] in mice using contrast enhanced MRI. Pharm Res. 2007, 24(6):1208-16.
[21] Xu R, Kaneshiro TL, Jeong EK, Parker DL, and Lu ZR, Synthesis and evaluation of nanoglobule-cystamine-(Gd-DO3A), a biodegradable nanosized magnetic resonance contrast agent for dynamic contrast-enhanced magnetic resonance urography, Int J Nanomedicine. 2010, 5:707-13.
[22] Tan M, Wu X, Jeong EK, Chen Q, Lu ZR., Peptide-Targeted Nanoglobular Gd-DOTA Monoamide Conjugates for Magnetic Resonance Cancer Molecular Imaging., Biomacromolecules. 2010, 11(3): 754-61
[23] Wu X, Jeong EK, Emerson L, Hoffman J, Parker DL, Lu ZR., Noninvasive Evaluation of Antiangiogenic Effect in a Mouse Tumor Model by DCE-MRI with Gd-DTPA Cystamine Copolymers. Mol Pharm. 2010: 7(1):41-8
[24] Wu X, Feng Y, Jeong EK, Emerson L, Lu ZR. Tumor characterization with dynamic contrast enhanced magnetic resonance imaging and biodegradable macromolecular contrast agents in mice., Pharm Res. 2009, 26(9):2202-8.
[25] Feng Y, Emerson L, Jeong EK, Parker DL, and Lu ZR, (2009), Application of a Biodegradable Macromolecular Contrast Agent in Dynamic Contrast-Enhanced MRI for Assessing the Efficacy of Indocyanine Green-Enhanced Photothermal Cancer Therapy. J Magn. Reson. Imag., 2009, 30(2):401-6.
[26] Ye Z, Jeong EK, Wu X, Tan M, Yin S, Lu ZR. Polydisulfide manganese(II) complexes as non-gadolinium biodegradable macromolecular MRI contrast agents. J Magn Reson Imaging. 2012;35(3):737-44.
[27] Liu X, Feng Y, Lu ZR, Morrell G, Jeong EK. Rapid simultaneous acquisition of T_1 and T_2 mapping images using multishot double spin-echo EPI and automated variations of TR and TE (ms-DSEPI-T12). NMR in biomedicine 2009.
[28] Liu X, Li KS, Jeong EK, Ocular pharmacokinetics study of corticosteroid by ^{19}F MR, Exp. Eye Research, 2010; 91: 347-352
[29] Li SK, Jeong EK, Hastings MS. Magnetic resonance imaging study of current and ion delivery into the eye during transscleral and transcorneal iontophoresis. *Invest Ophthalmol Vis Sci*, 2004, *45*(4), 1224-31.
[30] Li SK, Molokhia SA, Jeong EK. Assessment of subconjunctival delivery with model ionic permeants and magnetic resonance imaging. *Pharm Res*, 2004, *21*(12), 2175-84.
[31] Molokhia SA, Jeong EK, Higuchi WI, Li SK. Examination of barriers and barrier alteration in transscleral iontophoresis. J Pharm Sci. J Pharm Sci. 2008, 97(2):831-44.
[32] Liu X, Li KS, Jeong EK, Ocular pharmacokinetics study of corticosteroid by ^{19}F MR, Exp. Eye Research, 2010; 91: 347-352.
[33] Jiang ZX, Liu X, Jeong EK, Yu YB. Symmetry-guided design and fluorous synthesis of a stable and rapidly excreted imaging tracer for (19)F MRI. Angew Chem Int Ed Engl 2009;48(26):4755-4758.
[34] Jiang ZX, Yu YB. Fluorous mixture synthesis of asymmetric dendrimers. J Org Chem 2010;75(6):2044-2049.
[35] Tofts PS, Kermode AG. Measurement of the blood-brain barrier permeability and leakage space using dynamic MR imaging. 1. Fundamental concepts. Magn Reson Med 1991;17(2):357-367.

[36] Pintaske J, Martirosian P, Graf H, Erb G, Lodemann KP, Claussen CD, Schick F. Relaxivity of Gadopentetate Dimeglumine (Magnevist), Gadobutrol (Gadovist), and Gadobenate Dimeglumine (MultiHance) in human blood plasma at 0.2, 1.5, and 3 Tesla. Investigative radiology 2006;41(3):213-221.
[37] Shi XF, Kim SE, Jeong EK. Singleshot T_1 Mapping using Simultaneous Acquisitions of Spin- and STimulated-Echo Planar Imaging (2D ss-SESTEPI). Magn Reson Med, 2010; 64: 734-742.
[38] Jeong EK, Kim SE, Shi XF. SIMULTANEOUS ACQUISITIONS OF SPIN- AND SIMULATED-ECHO PLANAR IMAGING. US Patent Application No 12/392,072 2009.